Laser Light-Scattering Studies of Poly(caprolactone-*b*-ethylene oxide-*b*-caprolactone) Nanoparticles and Their Enzymatic Biodegradation

YUER ZHAO,[1] TENGJIAO HU,[1] ZE LV,[2] SHENGUO WANG,[2] CHI WU[1,3]

[1] Opening Laboratory for Bond-Selective Chemistry, Department of Chemical Physics, University of Science and Technology of China, Hefei, Anhui, People's Republic of China, 230026

[2] Laboratory of Membranes and Medical Polymers, Institute of Chemistry, Chinese Academy of Sciences, Beijing, People's Republic of China, 100080

[3] Department of Chemistry, Chinese University of Hong Kong, Shatin, NT, Hong Kong

Received 2 December 1998; revised 21 July 1999; accepted 9 August 1999

ABSTRACT: Water-insoluble triblock poly(caprolactone-*b*-ethylene oxide-*b*-caprolactone) (PCL-PEO-PCL) was micronized into narrowly distributed nanoparticles stable in water. Using a combination of static and dynamic laser light scattering (LLS), we characterized the resultant nanoparticles and studied their biodegradation in the presence of enzyme lipase PS. The results revealed that the biodegradation rate was mainly dependent on the enzyme concentration. The scattering intensity decreased as the degradation proceeded, but there was no change in size of the remaining nanoparticles, indicating that the degradation of each particle was fast and the enzyme consumed the nanoparticles individually. We also found that different copolymer compositions, i.e., different PCL–PEO molar ratios, led to different biodegradation rates. The pH and temperature dependence of the biodegradation rate were also studied. All results indicated that the biodegradation rate can be well controlled and the biodegradation essentially involves two processes: adsorption of lipase PS onto the nanoparticles, and enzymatic hydrolysis of the PCL blocks. The biomedical application of the enzymatic biodegradation of the copolymer nanoparticles is also envisioned. © 1999 John Wiley & Sons, Inc. J Polym Sci B: Polym Phys 37: 3288–3293, 1999

Keywords: triblock poly(caprolactone-*b*-ethylene oxide-*b*-caprolactone) copolymer; lipase PS; polymeric nanoparticles; enzymatic biodegradation; laser light scattering

INTRODUCTION

Biodegradable and biocompatible polymeric nanoparticles are of great interest because of their importance in biomedical applications and colloidal science, such as drug delivery devices and image-enhancing agents.[1,2] Commonly used biocompatible polymers are aliphatic polyesters, such as poly(ε-caprolactone) (PCL), poly(lactic acid) (PLA), poly(glycolic acid) (PGA), and their corresponding copolymers.[3] Special interest has been paid to their enzymatic biodegradation,[4–8] and biomedical applications.[9–11]

The micellization of block or graft copolymers in a selective solvent is one way to prepare polymeric nanoparticles.[12–15] The structures and applications of some biodegradable polymers have been reported,[16,17] including our previous study of poly(caprolactone) homopolymer.[18,19] Amphiphilic block copolymers with one or more poly(ethyl-

Correspondence to: C. Wu (E-mail: chiwu@cuhk.edu.hk)

Journal of Polymer Science: Part B: Polymer Physics, Vol. 37, 3288–3293 (1999)
 CCC 0887-6266/99/233288-06

Table I. Light-Scattering Characterization of Poly(caprolactone) Homopolymer (PCL100) and Poly(caprolactone-*b*-ethylene oxide-*b*-caprolactone) Triblock Copolymers in THF at 37°C

Sample	PCL100	PCL80	PCL60	PCL40
W_{PEO}/W_{PCL}	0/100	20/80	40/60	60/40
M_w/(g/mol)	1.43×10^5	7.30×10^4	7.50×10^4	4.75×10^4
$M_{w,PCL}$/(g/mol)	1.43×10^5	5.84×10^4	4.65×10^4	1.90×10^4
$M_{w,PEO}$/(g/mol)		1.46×10^4	2.85×10^4	2.85×10^4

ene oxide) (PEO) blocks are of special interest because PEO is biocompatible and unique for its low protein adsorption and low cell adhesion.[20–22]

In this study, we successfully micronized a water-insoluble triblock poly(caprolactone-*b*-ethylene oxide-*b*-caprolactone) (PCL-PEO-PCL) copolymer into a stable surfactant-free polymeric nanoparticle dispersion by adding the tetrahydrofuran (THF) solution of PCL-PEO-PCL dropwise into an excess of water. The laser light-scattering characterization showed that the nanoparticles made of the triblock copolymer had a cluster structure different from the uniform spherical structure made of the PCL homopolymer or even the diblock PEO-PCL copolymer. It is expected that hydrophobic drugs can be encapsulated inside the particles for biomedical application. In comparison with other degradation methods such as weighting or oxygen consumption, use of laser light scattering to study the biodegradation of formed nanoparticles in the presence of the enzyme lipase PS offers nonintrusive, accurate *in situ* measurement.

EXPERIMENTAL

Sample Preparation

Polycaprolactone and a series of PCL-PEO-PCL triblock copolymers were synthesized by polycondensation of a prescribed amount of ε-caprolactone (CL) (Janssen Chimica) and poly(ethylene glycol) (M_w = 1.46 × 10^4 or 2.85 × 10^4 g/mol) (Tianjin Eastern Health Materials Factory) at 160 °C in the presence of stannous octoate (Aldrich Chemical Company) as a catalyst for ~7 h. One PCL homopolymer and three copolymers were obtained and respectively denoted as PCL100, PCL80, PCL60, and PCL40, according their PCL percent contents which were determined by nuclear magnetic resonance imaging (NMR). Details of the polymerization can be found elsewhere.[23] The value of W_{PCL}/W_{PEO} and M_w are listed in Table I.

The triblock copolymers were micronized by adding 0.5 mL THF copolymer solution dropwise into 50 mL deionized water without stirring. The initial copolymer concentration in THF was 5.00 × 10^{-3} g/mL. THF immediately diffused into water when it was added into water, resulting in the collapsing and aggregation of the insoluble PCL blocks. The polymer aggregates were stabilized by the water-soluble PEO blocks acting as a hydrophilic shell. The technique of not stirring was used to reduce the interchain aggregation among the PCL blocks, so that smaller nanoparticles could be prepared. The final copolymer concentration in water was 4.95 × 10^{-5} g/mL, except where otherwise stated. For PCL100 (i.e., the homopolymer), cationic hexadecyltrimethylammonium bromide (HTAB) surfactant was added to stabilize the resultant nanoparticles.

Laser Light Scattering (LLS)

The LLS spectrometer is detailed elsewhere.[19] In static LLS, the angular dependence of the excess absolute time-averaged scattered intensity, that is, Rayleigh ratio, $R_{vv}(q)$, was measured. For a dilute solution at a relatively small scattering angle θ, $R_{vv}(q)$ can be related to the weight-averaged molar mass M_w, the second virial coefficient A_2, and the root-mean square z-averaged radius $\langle R_g^2 \rangle_z^{1/2}$ ($\langle R_g \rangle$) by[24]

$$\frac{KC}{R_{vv}(q)} \approx \frac{1}{M_w}\left(1 + \frac{1}{3}\langle R_g^2 \rangle_z q^2\right) + 2A_2C \qquad (1)$$

where $K = 4\pi^2(dn/dc)^2n^2/(N_A\lambda_0^4)$ and $q = (4\pi n/\lambda_0)\sin(\theta/2)$, with N_A, dn/dc, n, and λ_0 being Avogadro's number, the specific refractive index increment, the solvent refractive index, and the wavelength of light in vacuum, respectively. At $q \to 0$ and $C \to 0$, $R_{vv}(q) \sim KCM_w$.

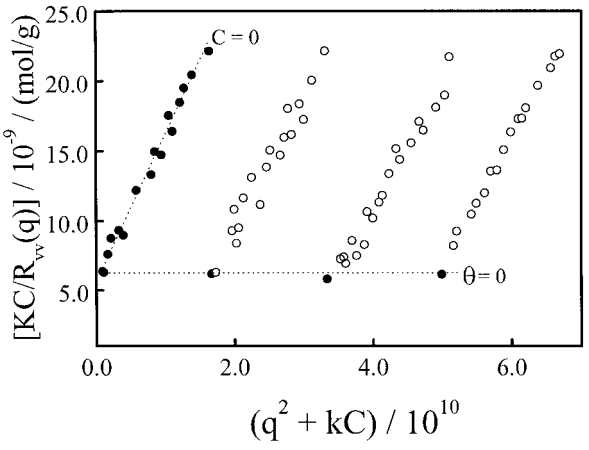

Figure 1. Typical Zimm plot of PCL60 nanoparticles in water at 37 °C, where the nanoparticle concentration ranged from 2.09×10^{-6} to 6.02×10^{-6} g/mL.

In dynamic LLS, the intensity–intensity time correlation function $G^{(2)}(t,q)$ in the self-beating mode was measured. The Laplace inversion of $G^{(2)}(t,q)$ resulted in a line-width distribution $G(\Gamma)$.[25] For a pure diffusive relaxation, Γ is related to the translational diffusion coefficient D by $\Gamma/q^2 = D$ at $q \to 0$ and $C \to 0$, so that $G(\Gamma)$ can be directly converted to the translational diffusion coefficient distribution G(D) or the hydrodynamic radius distribution $f(R_h)$ using the Stocks–Einstein equation: $R_h = k_BT/(6\pi\eta D)$ with k_B, T, and η being the Boltzman constant, absolute temperature, and solvent viscosity, respectively. Details of LLS instrumentation and theory can be found elsewhere.[24,25]

Enzymatic Biodegradation

Both PCL-PEO-PCL nanoparticle dispersion and the lipase PS aqueous solution were clarified by a 0.5-μm Millipore filter. In a typical enzymatic biodegradation experiment, a proper amount of dust-free lipase PS aqueous solution was added into 2 mL dust-free nanoparticle dispersion to start biodegradation. $R_{vv}(q)$ and $G^{(2)}(t,q)$ were simultaneously measured during enzymatic biodegradation. All biodegradation experiments were conducted *in situ* inside the LLS cuvette at T = 37 °C, except in the temperature dependence study.

RESULTS AND DISCUSSION

Figure 1 shows a typical Zimm plot of the PCL60 nanoparticles in water at 37 °C, which incorporates the angular and concentration extrapolations of $R_{vv}(q)$ on a single grid. On the basis of eq 1, the extrapolation of $[KC/R_{vv}(q)]_{C\to0,q\to0}$ led to M_w. The slopes of $[KC/R_{vv}(q)]_{C\to0}$ versus q^2 and $[KC/R_{vv}(q)]_{q\to0}$ versus C, respectively, led to $<R_g>$ and A_2. Note that $A_2 \sim 0$. The values of M_w and $<R_g>$ are summarized in Table II. It shows that the average number ($N_{aggregation}$) of the copolymer chains inside each nanoparticle is ca. 2300. As expected, $<R_g>$ decreased as the length of the PCL block decreased because the longer insoluble PCL block led to a stronger interchain aggregation.

Figure 2 shows a typical normalized hydrodynamic radius distributions $f(R_h)$ of the PCL60 nanoparticles in water at 37 °C, where $f(R_h)$ was calculated from the corresponding $G^{(2)}(q,t)$ using the Laplace inversion program CONTIN in the correlator. It shows that the PCL60 nanoparticles were narrowly distributed. The dynamic LLS results of all the PCL nanoparticles are also summarized in Table II, where the average hydrodynamic radius $<R_h>$ is defined as $\int f(R_h)R_h\, dR_h$. The nanoparticles had a ratio of $<R_g>/<R_h>$ much larger than the value (0.774) predicted for a uniform and nondraining sphere, indicating that

Table II. Light-Scattering Characterization of PCL Nanoparticles in Water at 37°C

Sample	PCL100	PCL80	PCL60	PCL40
$M_{w,particle}$/(g/mol)	3.31×10^8	1.71×10^8	1.59×10^8	1.23×10^8
$\langle R_g \rangle$/nm	95	116	108	74
$\langle R_h \rangle$/nm	103	96	85	66
$\langle R_g \rangle/\langle R_h \rangle$	0.92	1.21	1.27	1.12
$N_{aggregation}$	2300	2300	2100	2600
S_{chain}/nm^2		49	43	21

Relative errors: M_w, ±5%; $\langle R_g \rangle$, ±8%; $\langle R_h \rangle$, ±2%.

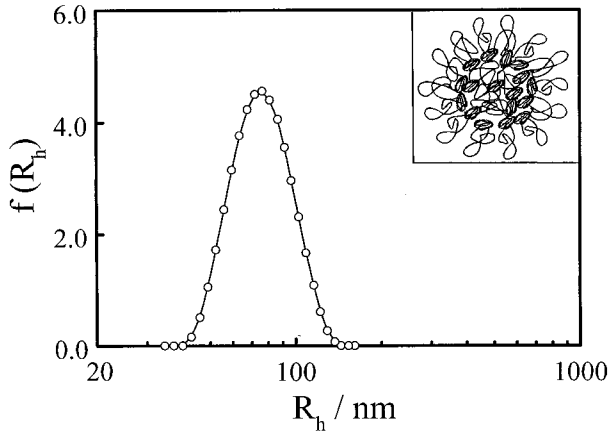

Figure 2. Typical normalized hydrodynamic radius distribution $f(R_h)$ of PCL60 nanoparticles in water at 37 °C. The inset shows a schematic of the PCL-PEO-PCL core-shell nanoparticle (cluster).

the PCL nanoparticles were hydrodynamically draining and had a loose cluster structure.

The PCL60 nanoparticles were stable for a long time and there was no size change in the temperature range studied. The surface area (S_{chain}) per copolymer chain, estimated from $<R_h>$ and the number of the copolymer chains inside each particle ($N_{aggregation}$) on the basis of $S_{chain} = 4\pi<R_h>^2/N_{aggregation}$ was in the range 20–60 nm^2. The values of S_{chain} were consistent with the radii (5–7 nm) of the collapsed PCL blocks. The inset in Figure 2 shows a schematic of the flower-like core-shell cluster structure, in which the collapsed and aggregated PCL blocks (the core) were stabilized by the swollen PEO shell.

The decrease in $[R_{vv}(q)]_t/[R_{vv}(q)]_0$ in Figure 3 indicates biodegradation. On the basis of eq 1, the decrease in $R_{vv}(q)$ can be attributed to a decrease in either the particle's molar mass (M_w) or polymer concentration (C). LLS could detect only the remaining PCL nanoparticles, not small biodegradation products (mainly five- and six-carbon acids). The time-independent average hydrodynamic radius $<R_h>$ of the remaining particles showed no change in the size of the remaining nanoparticles, that is, no change in M_w. Therefore, the decrease in $R_{vv}(q)$ can only be attributed to the decrease of C, so that $[R_{vv}(q)]_t/[R_{vv}(q)]_0 = C_t/C_0$. A combination of static and dynamic LLS results in Figure 3 indicates that the biodegradation of each nanoparticle must have been fast and lipase PS molecules consumed the nanoparticles one by one.

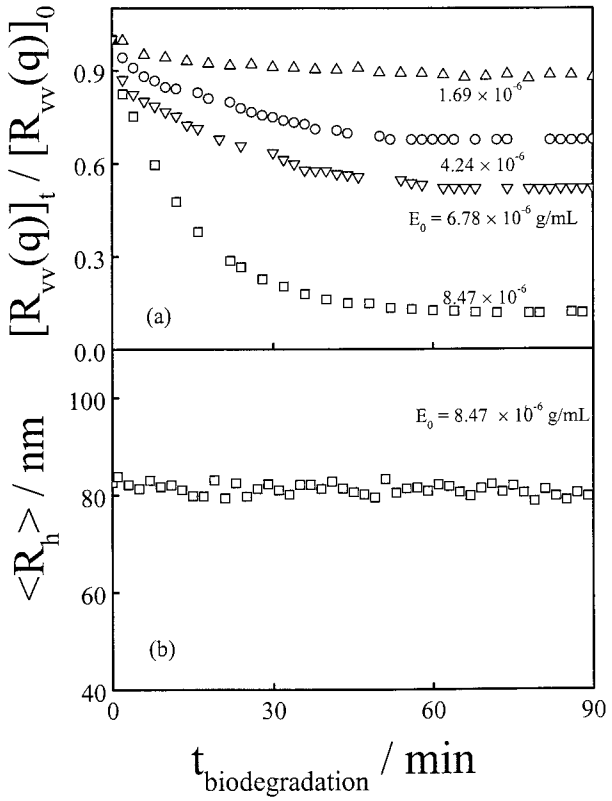

Figure 3. Biodegradation time dependence of the relative Rayleigh ratio $[R_{vv}(q)]_t/[R_{vv}(q)]_0$ and the average hydrodynamic radius $<R_h>$ of PCL60 nanoparticles at 37 °C, where subscripts "0" and "t" represent time $t = 0$ and $t = t$, respectively; and $C_0 = 4.95 \times 10^{-5}$ g/mL.

Figure 4 reveals that v_0 is a linear function of the enzyme concentration, and the line represents a least-square fitting of v_0 (μg/mL · min) = 0.12

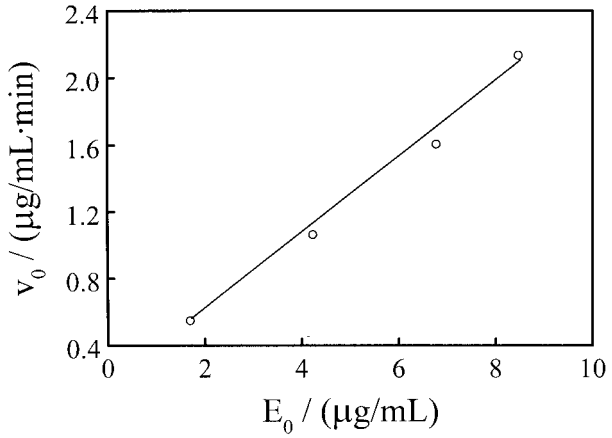

Figure 4. Enzyme concentration dependence of the initial biodegradation rate (v_0) of PCL60 nanoparticles at 37 °C, where $C_0 = 4.95 \times 10^{-5}$ g/mL and $v_0 = [dC_t/dt]_{t\to 0}$.

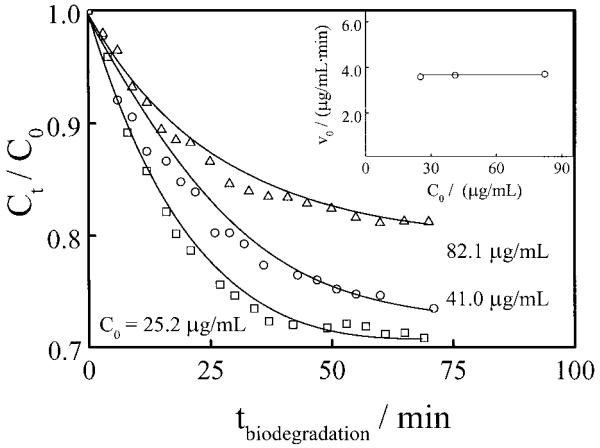

Figure 5. Initial copolymer concentration dependence of the relative polymer concentration (C_t/C_0) of PCL60 nanoparticles, where $E_0 = 8.47 \times 10^{-6}$ g/mL. The inset shows v_0 is nearly independent of the initial copolymer concentration.

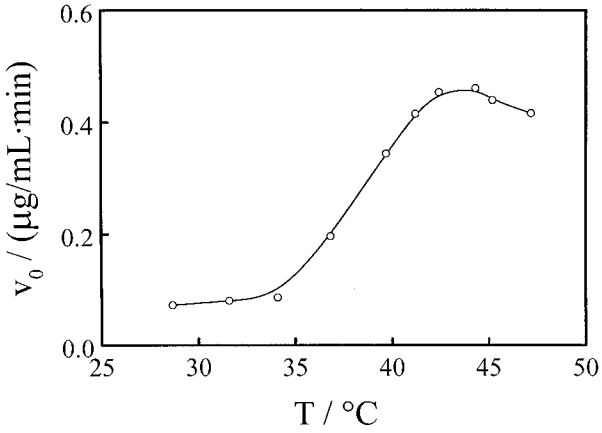

Figure 7. Temperature dependence of the initial biodegradation rate (v_0) of PCL60 nanoparticles, where $C_0 = 2.19 \times 10^{-5}$ g/mL and $E_0 = 2.72 \times 10^{-4}$ g/mL.

$+ 0.23E_0$. A combination of Figures 3 and 4 shows that not only v_0, but also the extent of the degradation increased as the enzyme concentration increased, indicating that lipase PS gradually lost its activity during biodegradation. Figure 5 shows that for a given lipase PS concentration E_0, v_0 was nearly independent of C_0. This is reasonable because if the biodegradation of the PCL nanoparticles occurs one by one, the number of the nanoparticles biodegraded per unit time should be dependent only on the number of lipase PS molecules.

Figure 6 shows that the normalized initial degradation rate (v_0) increased linearly as the PCL content increased despite the length of the PEO block. In a previous study of PCL homopolymers,[18,19] we observed that v_0 is a linear function of the PCL concentration for a given enzyme concentration. Figure 6 indicates that lipase PS can directly interact with the core made of PCL and the hydrophilic PEO shell has no effect on biodegradation. This can be attributed to the loose structure of the core-shell cluster—the cluster surface was not fully covered by the PEO blocks. We also studied the biodegradation of PLA in the presence of lipase PS and found no detectable change in both $R_{vv}(q)$ and $<R_h>$ although we varied the length of the PLA chains and the enzyme concentration, revealing that lipase PS can only hydrolyze PCL.

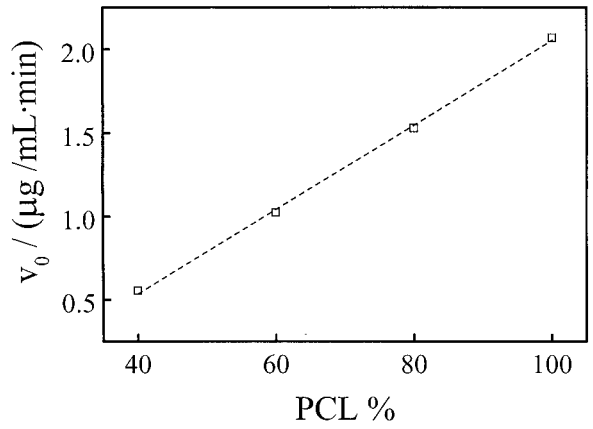

Figure 6. Copolymer composition dependence of the normalized initial biodegradation rate (v_0) at 37 °C, where $C_0 = 2.75 \times 10^{-5}$ g/mL and $E_0 = 1.56 \times 10^{-6}$ g/mL.

Figure 7 shows that the initial degradation rate increased as the temperature increased before reaching a maximum plateau at ~43 °C. In the temperature range 37–42 °C, ν_0 is a linear function of the temperature. Figure 8 reveals that when pH ≤ 5, the degradation was very slow, whereas in the range of pH = 5–9, the initial biodegradation rate increased linearly as pH increased, indicating that lipase PS was much more active at higher pH values. The temperature and pH dependence of the biodegradation rate can be envisioned in various biomedical applications, such as a body temperature-dependent drug release or a protecting matrix for drugs in the stomach, so that drugs can be released in a more basic environment of the intestines.

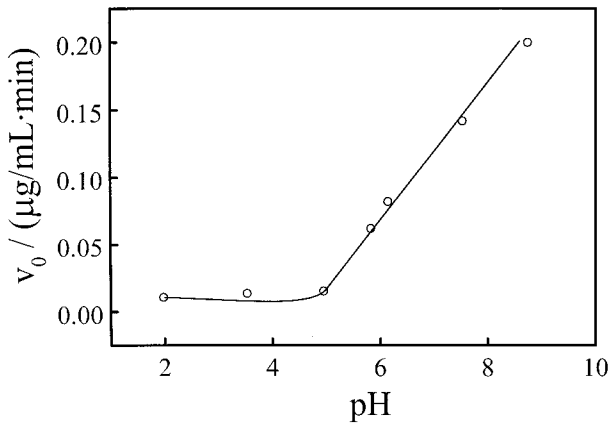

Figure 8. pH dependence of the initial biodegradation rate (v_0) of PCL60 nanoparticles at 37 °C, where $C_0 = 2.19 \times 10^{-5}$ g/mL and $E_0 = 2.72 \times 10^{-4}$ g/mL.

CONCLUSIONS

Insoluble PCL-PEO-PCL triblock copolymers can be micronized into small core-shell nanoparticles stable in water. Such resultant nanoparticles can undergo fast biodegradation in the presence of the enzyme lipase PS. The enzymatic biodegradation, monitored in terms of the scattering intensity (i.e., the polymer concentration in this case) and hydrodynamic size, reveals that the initial biodegradation rate mainly depends on the enzyme concentration, but not on the initial polymer concentration. This indicates that the biodegradation of each of nanoparticle is fast and the nanoparticles are consumed by lipase PS individually. Moreover, we found that the initial degradation rate increased as the length of the PCL block increased. The adjustable biodegradation rate by the enzyme concentration, the copolymer composition, pH, and temperature can be envisioned in various biomedical applications such as control-releasing devices. Research in this direction is ongoing.

Financial support of this work by the National Distinguished Young Investigator award (1996, 29625410) and the Research Grants Council of the Hong Kong Special Administration Region, Earmarked Grant 1997/98 (CUHK4181/97P, 2160082) is gratefully acknowledged.

REFERENCES AND NOTES

1. Schindler, A. Contemp Topic Polym Sci 1977, 2, 251.
2. Kelly, R. J. Rev Surg 1970, 2, 142.
3. Lewis, D. H. In Biodegradable Polymers as Drug Delivery Systems; Chassin, M.; Langer, R., Eds.; Marcel Dekker: New York, 1990; pp 1–41.
4. Huang, S. J. In Comprehensive Polymer Science; Allen, G.; Bevington, J. C., Eds.; Pergamon Press: New York, 1989; Chapter 21.
5. Kaplan, D. L.; Thomas, E. Technomic 1993, 1, 1.
6. Lenz, R. Adv Polym Sci 1993, 107, 3.
7. Swift, G. Acc Chem Res 1993, 26, 105.
8. Doi, Y. Microbial Polyesters; VCH: New York, 1990.
9. Chang, R. Physical Chemistry with Application to Biological Systems; Macmillan: New York, 1981; p 391.
10. Scholas, P. D.; Coombes, A. G. G.; Illum, L.; Davis, S. S.; Vert, M.; Davis, M.C. J Controll Rel 1993, 25, 145.
11. Lemoine, D.; Francois, C.; Kedzierwicz, F.; Preat, V.; Hoffman, M.; Maincent, P. Biomaterials 1996, 17, 2191.
12. Tuzer, Z.; Kratochvil, P. In Surface and Colloid Science, Vol. 15; Plenum Press: New York, 1993; pp 1–83.
13. Chu, B. Langmuir 1995, 11, 414.
14. Xu, R.; Winnik, M. Macromolecules 1991, 24, 87.
15. Liu, T.; Zhou, Z.; Wu, C.; Chu, B.; Schneider, D. K.; Nace, V. M. J Phys Chem B 1997, 101, 8808.
16. Gref, R.; Minamitake, Y.; Peracchia, M. T.; Trubetskov, V.; Langer, R. Science 1994, 263, 1600.
17. Hrkach, J. S.; Peracchia, M. T.; Domb, A.; Lotan, N.; Langer, R. Biomaterials 1997, 18, 27.
18. Gan, Z.; Jim, T. F.; Wu, C. Polymer 1998, 39, 4609.
19. Wu, C.; Gan, Z. Polymer 1998, 39, 4429.
20. Hermans, I. J Chem Phys 1982, 77, 2193.
21. Dolan, A. K.; Edwards, S. F. Proc R Soc Lond 1975, 343, 427.
22. Timmins, M. R.; Lenz, R. W.; Fuller, R. C. Polymer 1997, 55, 38.
23. Wang S.G.; Qin, B. Polym Adv Technol 1993, 4, 363.
24. Chu, B. Laser Light Scattering, 2nd ed.; Academic Press: New York, 1991.
25. Berne, B.; Pecora, R. Dynamic Light Scattering; Plenum Press: New York, 1976; pp 10–90.